Research Article

Benedikt Stender*, Fabian Hilbert, Yannick Dupuis, Alexander Krupp, Willi Mantei and Ruth Houbertz

Manufacturing strategies for scalable high-precision 3D printing of structures from the micro to the macro range

https://doi.org/10.1515/aot-2019-0022
Received February 15, 2019; accepted April 23, 2019; previously published online May 30, 2019

Abstract: Industrial high-precision 3D Printing (HP3DP) via two-photon absorption (TPA) provides freedom in design for the fabrication of novel products that are not feasible with conventional techniques. Up to now, 2PP-fabrication has only been used for structures on the micrometer scale due to limited traveling ranges of the translation stages and the field-of-view (FoV) of microscope objectives (diameters below 0.5 mm). For industrial applications, not only high throughput but also scalability in size is essential. For this purpose, this contribution gives insights into different manufacturing strategies composed of varying exposure modes, fabrication modes, and structuring modes, which enable the generation of large-scale optical elements without relying on stitching. With strategies like stage-only mode or synchronized movement of galvoscanners and translation stages, optical elements with several millimeters in diameter and freeform shape can be fabricated with optical surface quality.

Keywords: freeform; high-precision 3D printing; manufacturing strategy; scalable lenses.

1 Introduction

Since its demonstration in 1997 [1], high-precision 3D printing (HP3DP), also known as 3D lithography or fs direct laser writing (fs-DLW), gained attraction in a wide range of applications, such as photonics [2–5] microoptics [6], microfluidics [7], and life science [8, 9]. Its unique inherent 3D capability enables the fabrication of sophisticated components with unique designs and integrated functionalities [10–12]. Despite further development of commercially available printing platforms, HP3DP was only applied, so far, in the community for parts on the micro and mesoscale due to limited traveling ranges of used translation stages, the limited field-of-view (FoV) of focusing optics in combination with galvoscanners, and the way 3D structures are created in general, mostly resulting in extremely slow buildup rate. Objects larger than the FoV of the applied focusing optics are often stitched together, meaning that the structure is built step-by-step, where after each step, the sample or the focusing optics are moved instead of moving the laser beam with the galvoscanners. In many fabrication setups, this motion is coarser and/or less accurate than the motion of the laser beam within the FoV, resulting in an offset at the stitching joints [13]. However, even with accurate stages, stitching may introduce joints because the area that is processed during one step within an FoV is usually exposed in a short time compared to the time between multiple steps. The induced joints may have very disadvantageous effects, in particular for optical applications [14]. Post-processing may be suitable for some applications to reduce the effects of stitching [15]. For certain applications like direct fabrication on active and passive devices [16], post-processing may be difficult or even impossible.

Although there is a certain industrial need of sub-millimeter parts on an industrial scale, the demand for parts with a total size approaching the centimeter range is continuously increasing. This requirement can only be satisfied with novel manufacturing strategies comprised of different exposure modes, fabrication modes, and structuring modes as is demonstrated in this contribution. In addition, hybrid fabrication of combined manufacturing strategies enables the generation of large-area elements with adjustable printing resolution on-demand. HP3DP,

***Corresponding author: Benedikt Stender,** Multiphoton Optics GmbH, Friedrich-Bergius-Ring 15, Wuerzburg 97076, Germany, e-mail: benedikt.stender@multiphoton.de
Fabian Hilbert, Yannick Dupuis, Alexander Krupp, Willi Mantei and Ruth Houbertz: Multiphoton Optics GmbH, Wuerzburg, Germany

thus, closes the gap between conventional 3D printing technologies and micro- and nanofabrication technologies. It is an ideal tool for the fabrication of embedded and complex structures for replication masters in a single-process step and supports a fast prototyping phase for large optical elements (design iterations) to reduce time-to-market.

2 Experimental section

All objects shown in this paper were manufactured using the commercially available HP3DP equipment LithoProf3D (Multiphoton Optics GmbH, Germany). One out of two different objectives was selected for the fabrication of each object, depending on the required resolution and total size of the object. Structures with sub-micrometer feature size were fabricated using an oil immersion objective with high numerical aperture (NA 1.4) and 100-fold magnification. Larger objects were fabricated using an air objective with a lower numerical aperture (NA 0.6) and 40-fold magnification.

All objects were made from inorganic-organic hybrid polymers (ORMOCER®s) mainly ORMOCOMP® with 1 wt.% Lucirin TPO as photoinitiator. These materials allow high-resolution patterning, while they can be functionalized to adjust their optical properties [17]. For the fabrication an fs laser with a wavelength of 522 nm, a pulse-duration of 250 fs and a repetition rate of 63 MHz were applied. In order to move the focused laser light relative to the liquid photoresist, a system of air-bearing stages with a translation range of 10 cm × 10 cm × 5 cm or a galvoscanner was used. All structuring parameters were adjusted by the inhouse-developed 3D printing software LithoSoft3D. Slicing and hatching distances were in the range of 0.1–2 µm for the full-scan mode and 0.1–0.7 µm for the contouring mode; this mode was already published in the early days of TPA [1, 18]. In general, to achieve optical surface quality in the visible wavelength range, the slice and hatch distances should be chosen to sub-micrometer. For applications in the NIR to IR or non-optical use, coarser parameters can be used. Scanning speeds from 1 to 100 mm/s were used in combination with a variation in laser power from 2 to 50 mW, revealing the large process window of ORMOCER®s. After the exposure, the samples were developed with a mixture of isopropanol and methyl isobutyl ketone (3:1) for up to 10 min to remove the unexposed material. In case of a contouring structuring mode, the samples were illuminated with UV light after the development step for 10 s at about 25 mW/cm² to solidify the enclosed liquid polymer.

For characterization of the printed structures, a scanning electron microscope (TM3030, Hitachi) and a laser scanning microscope (LEXT OLS4000, Olympus) were used.

3 Manufacturing strategies

Depending on the structure's requirements, i.e. the desired dimension and printing resolution, an adaptation of the corresponding manufacturing strategy is necessary. This contains a suitable modification of the exposure mode, fabrication mode, and structuring mode.

The exposure mode summarizes the optics (numerical aperture and working distance) focusing the fs laser light into the sample as well as the workpiece configuration with respect to the microscope objective and includes factors like penetration distance through a photoactive material to the substrate to be processed on. In standard 3D lithography (see Figure 1A), microscope objectives with a high numerical aperture provide a higher printing resolution than objectives with a low numerical aperture, as the laser light can be focused more tightly. In a setup where the objective is moved in vertical direction while the object itself is moved only in lateral direction, the working distance of an objective sets an upper limit of the maximum possible printing height. High numerical aperture immersion objectives, however, inherently possess low working distance and, thus, limit the achievable printing height to some hundred micrometers. This limitation can partially be overcome to some millimeters using the photoresist as immersion media by dipping the

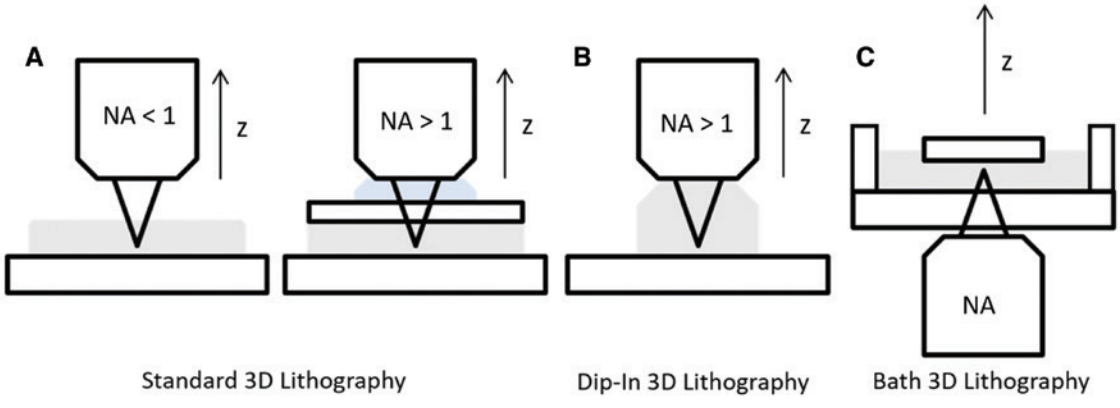

Figure 1: Exposure modes applied for HP3DP: (A) standard 3D lithography, (B) dip-in 3D lithography, and (C) bath 3D lithography.

microscope objective into the liquid material (dip-In 3D lithography, see Figure 1B), as was shown by Stichel et al. (2010) [19] and Bückmann et al. (2012) [20]. An additional expansion of the available on-axis printing height to the centimeter range (depending on the travelling range of the mounted axis) is provided by inverted focusing of the laser light into a bath configuration with a fixed position of the focal point along the optical axis and gradually pulling out the substrate out of the bath [21, 22] (bath 3D lithography, see Figure 1C).

The fabrication mode defines the relative movement of the focal point through the material. Conventionally, high-precision piezo translation stages are applied to move the sample with respect to the focal point [1] but coming along with limited traveling range and scans peed [23]. Alternatively, air-bearing stages with lower accuracy are used. However, the difference in accuracy is to no extent noticeable in the HP3DP process as the voxel dimensions are in any case more pronounced [2, 24, 25]. On the contrary, air-bearing stages have the advantage of long traveling ranges enabling stitching-free manufacturing. In the following, the fabrication via a movement of the sample with respect to a fixed focal point is referred to as the stage-only mode (Figure 2A). For each structure, there exists an optimum writing speed v_{opt}, which is dependent on the acceleration a and line length l according to

$$v_{opt} = \sqrt{\frac{1}{2} al}$$

This scan speed v_{opt} results in a minimum printing time for a specific line length and can be derived by the physics of motion.

As translation stages exhibit a high inertia, the acceleration is limited. Thus, fabrication using a galvo mode (see Figure 2B) with galvoscanners containing high-frequency mirrors enable higher processing speeds [25]. Although the fabrication time can be reduced by applying the galvo mode, the accessible scan area is limited to the field-of-view (FoV) of the respective microscope objective, which is only several hundred micrometers (typically below 0.5 mm) [26]. In principle, low-numerical aperture objectives with a low magnification can be used, but these drastically reduce the possible printing resolution [23]. Structures much more pronounced than the FoV of an objective can, in general, be fabricated by stitching [13], which, however, leads to joints that are especially unfavorable for optical elements as aberrations (scattering, refraction, etc.) are induced by these artifacts [14]. Synchronizing the movement of translation stages and galvoscanners with respect to each other (synchronized mode enabled by the controller, see Figure 2C) enlarges the scan field of the galvoscanner to the entire traveling range as the simultaneous movement of the traveling stage continuously shifts the FoV [27]. In addition, it reduces positioning errors.

The structuring mode implies the scanning trajectory of the focal volume to fabricate an object, as shown in Figure 3. Typically, a full-volume scanning by slicing and hatching is used, which can be very time intensive, particularly if larger parts or large arrays of elements should be fabricated. By contouring the outer shell of an object, for example, a lens, the production time can be reduced by up to 95% [25, 28]. The residual liquid photoresist enclosed between cross-linked shell and substrate is subsequently polymerized with a UV illumination after the development step. By μ-Raman spectroscopy, it was shown that this procedure results in very homogeneous organically cross-linked materials with no variation in the homogeneity [29]. Using this structuring mode, the fabrication time of a lens with a diameter of 100 μm and a height of 20 μm can be as low as 1 s per lens in a serial production [28]. The achieved surface roughness of Ra = 20–30 nm is still suitable for optical applications in the visible spectral range [30, 31]. It has to be mentioned, however, that parallel

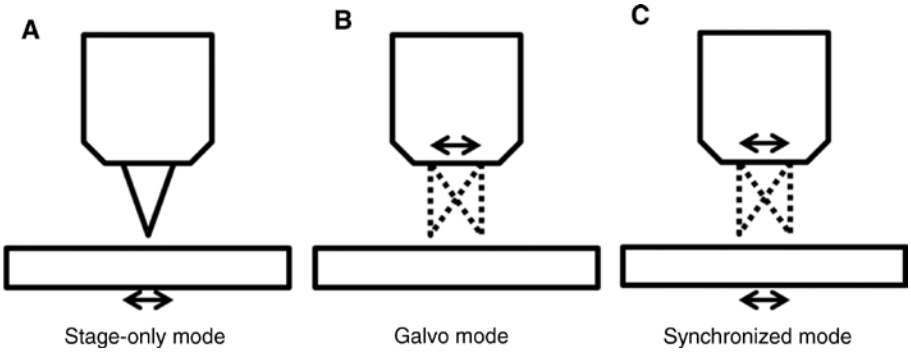

Figure 2: Fabrication modes using HP3DP: (A) stage-only mode, (B) galvo mode, and (C) synchronized mode.

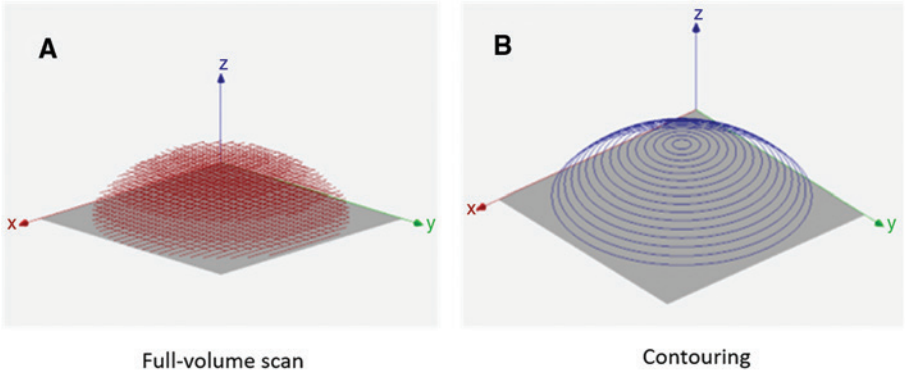

Figure 3: Structuring modes for HP3DP: (A) full-volume scan and (B) contouring.

fabrication of structures is also easily achievable, allowing to even more decrease the fabrication times.

4 Manufacturing of macro elements

Sub-micrometer printing resolution of HP3DP is effortlessly achieved using high numerical immersion objectives in combination with exposure modes close to the optical design case of the objective. This means that the penetration depth is supposed to be as small as possible as induced aberrations increase with increasing penetration depth [21]. A variation of sub-micrometer structures is shown in Figure 4A. For parts on the centimeter scale, this fabrication approach is not suitable. To create elements on the macro scale, the bath 3D lithography exposure mode in combination with the stage-only fabrication mode is suitable. For the 2 cm × 2 cm airscrew displayed in Figure 4B, a full-volume fabrication mode with a coarser printing resolution was chosen. A comparison of Figure 4A and B demonstrates the scalability of HP3DP over 5 orders of magnitude, and it is a very good example that this technology closes the gap between nano- or microfabrication and conventional 3D printing technologies.

The fabrication of large-scale optical elements with high surface quality is a more challenging task. In general, one can simply print with a high-resolution full-volume structuring mode in combination with a stage-only fabrication mode. However, this ends up in uneconomic fabrication times of days to years. For this reason, the contouring fabrication mode is a suitable way in order to fabricate millimeter-sized lenses as shown in Figure 4C. This fabrication mode is not only limited to spherical profiles but also can be applied to create freeforms as shown in Figure 4D. For demonstration of the functionality of the fabricated millimeter lenses, an array is placed onto a computer screen magnifying the individual pixel colors (see Figure 4E). An example of a large-area scaffold structure is displayed in Figure 4F. The size of the woodpile is 1.5 mm × 1.5 mm with the individual layers structured via synchronized fabrication mode. The printing time of this structure was 50 min.

The great advantage of HP3DP is the possibility of applying a hybrid manufacturing strategy for complex structures consisting of different elements in a single-process step. Depending on the corresponding requirements on shape accuracy and surface finish, each part can be manufactured with different fabrication modes and structuring modes with a printing resolution on demand. This is shown in Figure 5 for a lens with a diameter of 1 mm embedded into a frame structure 1.5 × 1.5 mm in size with alignment features. This design resembles an element used in mastering for replication processes. The alignment features can be used for plugging of two opposed counterparts. The lens was manufactured by a contoured structuring mode, and the frame was created using full-volume structuring mode via stage-only fabrication. For the entire system, the same exposure mode was applied. It has to be mentioned that one can easily modify the exposure mode (and the material) in between the different structuring strategies.

A more pronounced processing area of 7.5 mm × 7.5 mm with a variety of elements is demonstrated in Figure 6A. The rectangular base element includes branding elements to prevent counterfeit consumer goods or for security reasons (Figure 6B), cross-markers and holes as alignment features (Figure 6C), which were *in situ* fabricated. As high-speed stage-only fabrication mode at a scanning speed of 30 mm/s in combination with a full-volume structuring mode was used for manufacture to avoid supporting structures, these integrated elements imply a high time accuracy of triggering the laser. By changing the fabrication mode to a synchronized mode as well as the structuring mode to contouring, not only large lenses with a diameter of 2 mm are manufactured (Figure 6D) but also

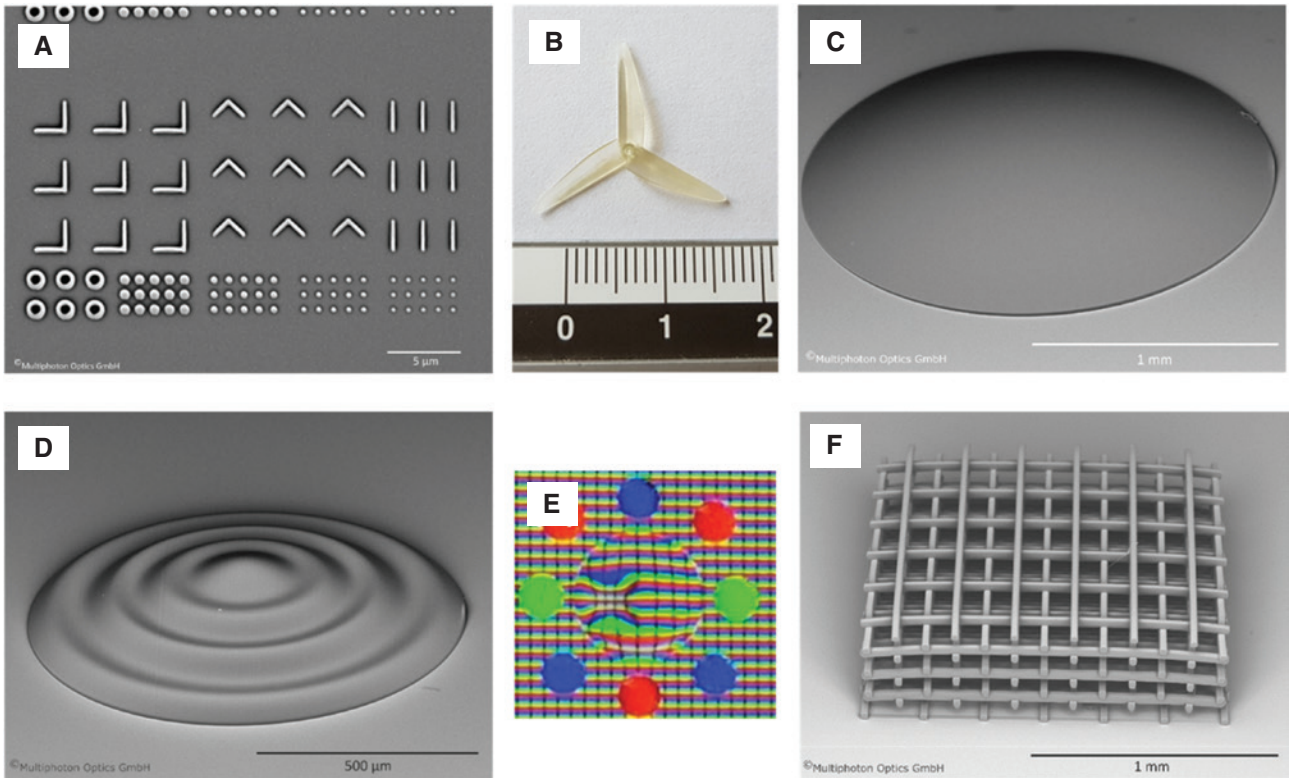

Figure 4: Examples of different structures fabricated in different manufacturing strategies: (A) sub-micrometer elements fabricated utilizing a high-numerical aperture microscope objective and a laser beam movement according to galvo fabrication mode; (B) centimeter-sized airscrew structure created via bath 3D lithography and a stage-only fabrication mode; (C) lens with a diameter of 1 mm fabricated with a stage-only fabrication mode in combination with structuring via contouring; (D) Freeform millimeter-sized lens with the same manufacturing strategies as in (C); (E) magnification of individual pixel colors of a computer screen with a lens array; (F) Large-area scaffold structure created via a synchronized fabrication mode.

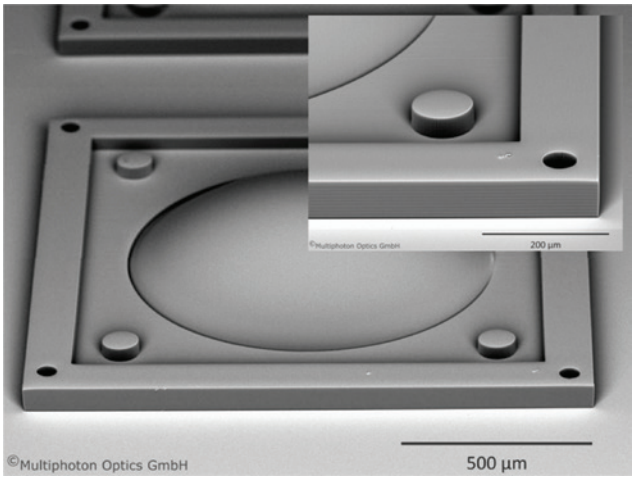

Figure 5: Hybrid fabrication of a complex element consisting of a 1-mm lens embedded into a frame. Both elements were fabricated in a one-step process but with different structuring modes (contouring for the lens, full volume for the frame).

grating structures (Figure 6E) without the need to stitch or change the workpiece during manufacturing. By serial fabrication only, the entire printing time for the element in Figure 6 summed up to 72 h. In prospective works, this time is supposed to be reduced tremendously by parallelization using multiple focal spots.

5 Surface roughness and shape deviation

The surface quality of a contoured lens with a diameter of one millimeter is evaluated with a laser scanning microscope (50× objective and 20× objective). As depicted in Figure 7A, the two-dimensional height map reveals homogeneous height levels. The correspondingly determined line profile roughness for two different line lengths (250 µm and 600 µm) amounts to Ra = 10–20 nm and Rq = 10–30 nm. For an area of 250 × 250 µm², the surface roughness was determined to be Sa = 12 nm and Sq = 15 nm, respectively, which is perfectly suitable for optical applications. In order to obtain more statistical data, future work will include collection of data on a set of different lenses and more pronounced areas.

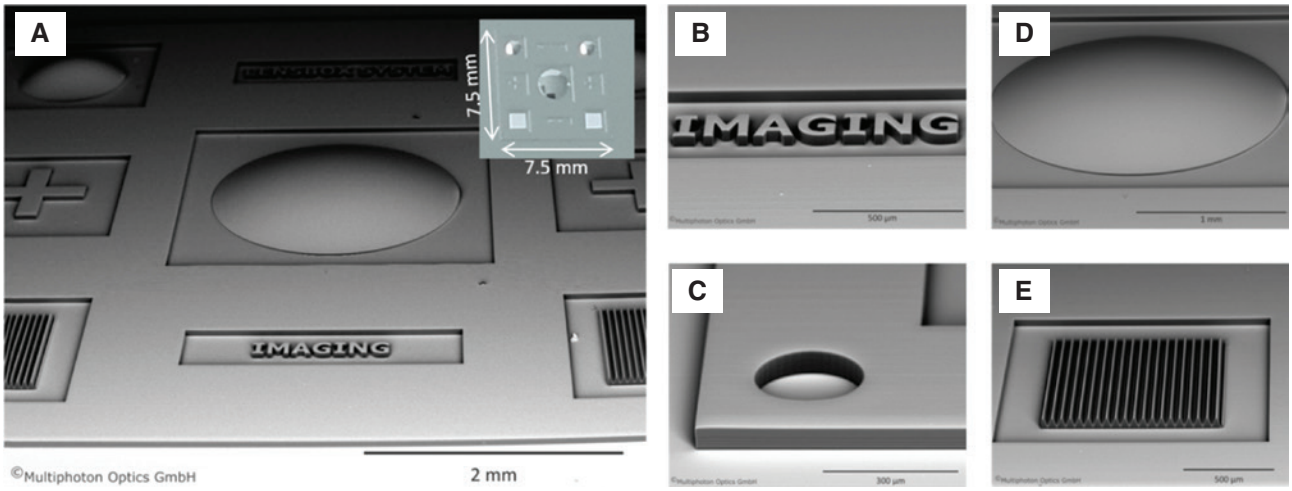

Figure 6: Example for hybrid manufacturing of a 7.5 mm × 7.5 mm complex structure with integrated features and optical elements: (A) SEM image at lowest possible magnification and a photography of the entire structure in the inset; integrated features like (B) text or (C) alignment features enable branding and applications for replication and/or molding. Optical elements as (D) a lens with a diameter of 2 mm, or (E) grating structures can be implemented in a one-step process only by changing the structuring mode.

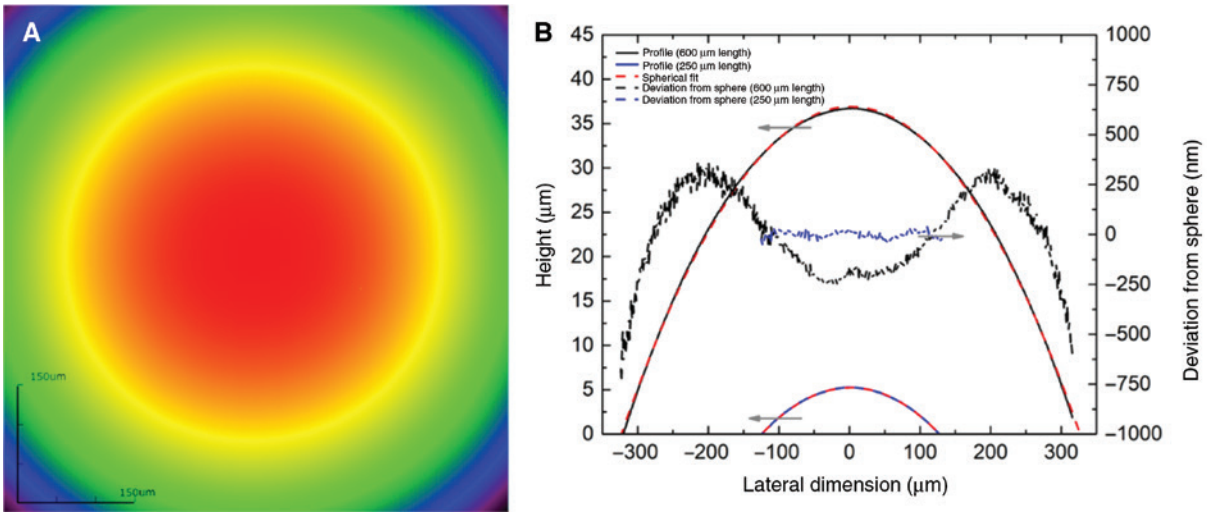

Figure 7: Surface quality of a fabricated lens with a diameter of 1 mm. (A) Two-dimensional height profile with homogeneous height levels. (B) Measured profiles and shape deviation with respect to a fitted spherical shape.

As the design shape of the lens was of spherical nature, the profile was fitted with a spherical shape (see red dotted line in Figure 7B) for two different profile lengths of 250 µm and 600 µm (50× objective and 20× objective, respectively) to investigate the resulting change in natural shape induced by the fabrication of a 3D object by lateral contouring lines. The correspondingly determined deviation of the not yet fully optimized shape from the fitted spherical shape ranges between ±500 nm, demonstrating the preservation of shape nature of the combined process of contouring with two-photon polymerization and subsequently applied UV illumination indicating that simple strategies (like profile iteration) are sufficient to compensate for shape deviations from the theoretical design due to shrinkage effects. For the central part of the lens (125 µm distance to the lens` sag), the shape accuracy is even within ±100 nm.

6 Summary

In conclusion, we gave insights into the different manufacturing strategies using HP3DP. These were composed of different exposure modes, fabrication modes, and

structuring modes, each influencing factors like printing resolution, printing height, accessible printing area, scanning speed, and surface finish that have to be considered prior to printing. With suitable fabrication modes like stage-only or synchronized mode, fabrication of large optical elements is feasible without stitching. Although a full-volume structuring mode is typically applied in the community, it is not reasonable for large optics or, more generally, for elements with sizes larger than the FoV. For this purpose, a contouring structuring mode reduces the printing time with almost similar surface finish. With hybrid manufacturing strategies, complex workpieces with different elements can be fabricated with a printing resolution on demand in a one-step process, as was shown for large lenses with up to 3 mm in diameter, large area gratings, and frames with implemented alignment features. For large optical elements like lenses fabricated with a contouring structuring mode, the line roughness ranging from 10 to 30 nm is suitable for imaging and illumination applications. The described process of contouring is capable of preserving the original design shape and does not require intensive shape corrections and adaptations. It is, therefore, ideally suitable for the fabrication of freeform shapes. After the demonstration of printability, future work will include an optimization with respect to printing time.

Funding: Part of the work was funded by Bundesministerium für Wirtschaft und Energie, Funder Id: http://dx.doi.org/10.13039/501100006360, Grant Number: TOU-1512-004.

References

[1] S. Maruo, O. Nakamura and S. Kawata, Opt. Lett. 22, 132 (1997).
[2] J. Serbin, A. Egbert, A. Ostendorf, B. N. Chichkov, R. Houbertz, et al. Opt. Lett. 28, 301 (2003).
[3] R. Houbertz, H. Wolter, V. Schmidt, L. Kuna, V. Satzinger, et al. MRS Proc. 1054, 1054-FF01-04 (2007).
[4] J. K. Gansel, M. Thiel, M. S. Rill, M. Decker, K. Bade, et al., Science 325, 1513–1515 (2009).
[5] A. I. Aristov, M. Manousidaki, A. Danilov, K. Terzaki, C. Fotakis, et al. Sci. Rep. 6, 1–8 (2016).
[6] T. Gissibl, S. Thiele, A. Herkommer and H. Giessen, Nat. Photonics 10, 554–560 (2016).
[7] S. M. Eaton, C. De Marco, R. Martinez-Vazquez, R. Ramponi, S. Turri, et al. J. Biophotonics 5, 687–702 (2012).
[8] T. Stichel, B. Hecht, R. Houbertz and G. Sextl, J. Laser Micro Nanoeng. 5, 209–212 (2010).
[9] F. Böhrnsen, M. Krier, S. Grohmann, N. Hauptmann, M. Frant, et al. Biomed. Mater. 14, 035001 (2019).
[10] M. Farsari, M. Vamvakaki and B. N. Chichkov, J. Opt. 12, 124001 (2010).
[11] D. Wu, S. Z. Wu, J. Xu, L. G. Niu, K. Midorikawa, et al. Laser Photonics Rev. 8, 458–467 (2014).
[12] L. Jonušauskas, S. Rekštytė, R. Buividas, S. Butkus, R. Gadonas, et al. Opt. Eng. 56, 1 (2017).
[13] S. Dehaeck, B. Scheid and P. Lambert, Addit. Manuf. 21, 589–597 (2018).
[14] J. Li, P. Fejes, D. Lorenser, B. C. Quirk, P. B. Noble, et al. Sci. Rep. 8, 1–9 (2018).
[15] N. Chidambaram, R. Kirchner, R. Fallica, L. Yu, M. Altana, et al. Adv. Mater. Technol. 2, 1700018 (2017).
[16] P. I. Dietrich, M. Blaicher, I. Reuter, M. Billah, T. Hoose, et al. Nat. Photonics 12, 241–247 (2018).
[17] R. Houbertz, G. Domann, C. Cronauer, A. Schmitt, H. Martin, et al. Thin Solid Films 442, 194–200 (2003).
[18] J. Serbin, R. Houbertz, C. Fallnich and B. N. Chichkov, Laser Micromach. Optoelectron. Device Fabr. 4941, 73 (2003).
[19] T. Stichel, R. Houbertz and B. Hecht, in: '11th International Symposium on Laser Precision Microfabrication', 2010.
[20] T. Bückmann, N. Stenger, M. Kadic, J. Kaschke, A. Frölich, et al. Adv. Mater. 24, 2710–2714 (2012).
[21] T. Stichel, B. Hecht, S. Steenhusen, R. Houbertz and G. Sextl, Opt. Lett. 41, 4269 (2016).
[22] T. Stichel, Die Herstellung von Scaffolds aus funktionellen Hybridpolymeren für die regenerative Medizin mittels Zwei-Photonen-Polymerisation (University Library Würzburg, Würzburg, 2014). http://publica.fraunhofer.de/dokumente/N-426462.html.
[23] X. Zhou, Y. Hou and J. Lin, AIP Adv. 5, 030701 (2015).
[24] K. S. Lee, R. H. Kim, D. Y. Yang and S. H. Park, Prog. Polym. Sci. 33, 631–681 (2008).
[25] H. Sun and S. Kawata, J. Light. Technol. 21, 624–633 (2003).
[26] M. Malinauskas, H. Gilbergs, A. Ukauskas, V. Purlys, D. Paipulas, et al. J. Opt. 12, 035204 (2010).
[27] L. Jonušauskas, D. Gailevičius, L. Mikoliunaite, D. Sakalauskas, S. Šakirzanovas, et al. Materials (Basel) 10, 1–18 (2017).
[28] B. Stender, W. Mantei, R. Houbertz and B. Hall, Laser Tech. J. 14, 20–23 (2017).
[29] S. Steenhusen, Untersuchungen zur sub-100 nm Strukturierung von Hybridpolymeren mittels Zwei-Photonen Absorption und Anwendungen (Friedrich-Schiller-Universität Jena, Jena, Germany, 2018). http://publica.fraunhofer.de/documents/N-519861.html.
[30] M. Born and E. Wolf, 'Principles of Optics', 6th edition (Pergamon Press, Oxford, 1980).
[31] S. Sinzinger and J. Jahns, 'Microoptics', (Wiley-VCH Verlag GmbH & Co. KGaA, Weinheim, 2003).